The proteasome inhibitor bortezomib interacts synergistically with histone deacetylase inhibitors to induce apoptosis in Bcr/Abl$^+$ cells sensitive and resistant to STI571

Chunrong Yu, Mohamed Rahmani, Daniel Conrad, Mark Subler, Paul Dent, and Steven Grant

Interactions between the proteasome inhibitor bortezomib and histone deacetylase inhibitors (HDIs) have been examined in Bcr/Abl$^+$ human leukemia cells (K562 and LAMA 84). Coexposure of cells (24-48 hours) to minimally toxic concentrations of bortezomib + either suberoylanilide hydroxamic acid (SAHA) or sodium butyrate (SB) resulted in a striking increase in mitochondrial injury, caspase activation, and apoptosis, reflected by caspases-3 and -8 cleavage and poly(adenosine diphosphate–ribose) polymerase (PARP) degradation. These events were accompanied by down-regulation of the Raf-1/mitogen-induced extracellular kinase (MEK)/extracellular signal-related kinase (ERK) pathway as well as diminished expression of Bcr/Abl and cyclin D_1, cleavage of p21^{CIP1} and phosphorylation of the retinoblastoma protein (pRb), and induction of the stress-related kinases Jun kinase (JNK) and p38 mitogen-activated protein kinase (MAPK). Transient transfection of cells with a constitutively active MEK construct significantly protected them from bortezomib/SAHA-mediated lethality. Coadministration of bortezomib and SAHA resulted in increased reactive oxygen species (ROS) generation and diminished nuclear factor κB (NF-κB) activation; moreover, the free radical scavenger L-N-acetylcyteine (LNAC) blocked bortezomib/SAHA-related ROS generation, induction of JNK and p21^{CIP1}, and apoptosis. Lastly, this regimen potently induced apoptosis in STI571 (imatinib mesylate)–resistant K562 cells and CD34$^+$ mononuclear cells obtained from a patient with STI571-resistant disease, as well as in Bcr/Abl$^-$ leukemia cells (eg, HL-60, U937, Jurkat). Together, these findings raise the possibility that combined proteasome/histone deacetylase inhibition may represent a novel strategy in leukemia, including apoptosis-resistant Bcr/Abl$^+$ hematologic malignancies. (Blood. 2003;102:3765-3774)

Introduction

The Bcr/Abl oncogene encodes a fusion protein that is found in the cells of 95% of patients with chronic myelogenous leukemia (CML).[1] Constitutive activation of the Bcr/Abl tyrosine kinase contributes to leukemic transformation[2] and has been shown to render such cells highly resistant to apoptosis induced by noxious stimuli, including cytotoxic drugs, compared with Bcr/Abl leukemic cells.[3,4] Multiple signaling/survival pathways downstream of Bcr/Abl have been implicated in this phenomenon, including those related to nuclear factor κB (NF-κB), signal transducer and activator of transcription 5 (Stat5), mitogen-induced extracellular kinase (MEK)/mitogen-activated protein (MAP) kinase, Bcl-x_L, and Akt, among others.[5-9] The identification of Bcr/Abl as the pathophysiologic lesion of CML prompted the development of STI571, a tyrosine kinase inhibitor that inhibits the Bcr/Abl, c-Kit, and to a lesser extent, other kinases.[10] STI571(imatinib mesylate; Gleevec) inhibits the growth of and induces apoptosis in Bcr/Abl-positive leukemia cells in vitro[11,12] and has proved to be highly active, when administered orally in patients with CML.[13] However, the emergence of STI571 resistance in CML patients initially responsive to this agent[14] has led to the search for additional approaches to the treatment of this disease.

Proteasome inhibitors represent a relatively new class of antineoplastic agents that act by interfering with the catalytic 20S core of the proteasome, thereby preventing the elimination of diverse cellular proteins targeted for degradation.[15] There are several classes of proteasome inhibitors including peptide aldehydes such as MG-132,[16] as well as the dipeptidyl boronic acid bortezomib (Velcade, formerly known as PS-341; Millenium Pharmaceuticals, Cambridge, MA), which is a more specific inhibitor of the proteasome.[17] For reasons that are incompletely understood, proteasome inhibitors effectively induce apoptosis in tumor cells, but are relatively sparing of their normal counterparts.[18] Of the many cellular perturbations induced by proteasome inhibitors, interference with NF-κB signaling has been the subject of intense scrutiny.[19] Interest in the clinical development of proteasome inhibitors has been sparked by recent findings indicating that bortezomib exhibits significant activity in patients with multiple myeloma.[20] Currently, the clinical utility of proteasome inhibitors in leukemia in general, and in CML in particular, remains relatively unexplored.

Histone deacetylase inhibitors (HDIs) constitute a diverse group of compounds that promote histone acetylation, chromatin uncoiling, and transcription of a variety of genes involved in multiple cellular processes, including differentiation.[21] In addition, histone

From the Departments of Medicine, Radiation Oncology, Biochemistry, Microbiology, Human Genetics, and Pharmacology, Virginia Commonwealth University, Medical College of Virginia, Richmond, VA.

Submitted March 12, 2003; accepted July 9, 2003. Prepublished online as *Blood* First Edition Paper, August 7, 2003; DOI 10.1182/blood-2003-03-0737.

Supported by awards CA63753-05, CA83705, CA93738, and CA100866 from the National Cancer Institute, National Institutes of Health (NIH); award 6045-03 from the Leukemia and Lymphoma Society of America; and award DAMD-03-1-0209 from the Department of Defense, U.S.A. Medical Research and Medical Command.

Reprints: Steven Grant, Division of Hematology/Oncology, Medical College of Virginia/Virginia Commonweatlth University, MCV Station Box 230, Richmond VA, 23298; e-mail: stgrant@hsc.vcu.edu.

The publication costs of this article were defrayed in part by page charge payment. Therefore, and solely to indicate this fact, this article is hereby marked "advertisement" in accordance with 18 U.S.C. section 1734.

deacetylase inhibitors can also induce apoptosis, particularly in leukemic cells, through a process regulated by induction of the cyclin-dependent kinase inhibitor $p21^{CIP1}$ (Rosato et al[22]) or generation of reactive oxygen species (ROS).[23] In K562 cells, HDIs, when administered at low, relatively nontoxic concentrations, induce maturation along the erythroid lineage.[24] While several HDIs, including suberoylanilide hydroxamic acid (SAHA), depsipeptide, and members of the short chain fatty acid butyrate family (eg, phenylbutyrate) have undergone clinical evaluation,[25-27] their role in the treatment of CML remains to be defined.

Previous studies have indicated that exposure of tumor cells to HDIs such as phenylbutyrate leads to inactivation of NF-κB.[28] Such findings raise the possibility that coadministration of HDIs with proteasome inhibitors, which also interrupt this pathway,[19] might be associated with enhanced antitumor activity. Currently, no information is available concerning interactions between clinically relevant HDIs and proteasome inhibitors in leukemia cells in general, and Bcr/Abl$^+$ leukemia cells in particular. To address this issue, we have examined the effects of treatment of Bcr/Abl$^+$ cells (K562 and LAMA 84), including those resistant to STI571, with HDIs in combination with the proteasome inhibitor bortezomib. Here we report that these agents interact in a highly synergistic manner to induce mitochondrial injury, caspase activation, and apoptosis in Bcr/Abl$^+$ cells, and that these events are associated with multiple perturbations in signaling and survival pathways, including inhibition of $p21^{CIP1}$ induction, potentiation of Jun kinase (JNK) phosphorylation, and interference with NF-κB DNA binding. Moreover, the HDI/bortezomib regimen potently induces apoptosis in continuously cultured and primary Bcr/Abl$^+$ cells that are resistant to STI571, as well as in Bcr/Abl$^-$ leukemic cells. Together, these findings suggest that an approach combining clinically relevant HDIs with proteasome inhibitors warrants further investigation as a therapeutic strategy for both Bcr/Abl$^-$ leukemias as well as those that are Bcr/Abl$^+$ and otherwise resistant to standard cytotoxic agents.

Materials and methods

Cells

K562 cells were purchased from American Type Culture Collection (Rockville, MD). LAMA 84 cells were purchased from the German Collection of Microorganisms and Cell Cultures (Braunschweig, Germany). All were cultured in RPMI 1640 supplemented with sodium pyruvate, minimum essential medium (MEM), essential vitamins, L-glutamate, penicillin, streptomycin, and 10% heat-inactivated fetal calf serum (FCS; Hyclone, Logan, UT). Multidrug-resistant K562 cells (K562R), which display approximately a 4-fold increase in levels of the Bcr/Abl protein and are approximately 10-fold more resistant to STI571 than the parental line, were derived and maintained as described in detail previously.[29] Cells were cultured in the absence of all drugs for at least 2 days prior to experimental procedures.

CD34$^+$ cells were obtained with informed consent from peripheral blood from a patient with accelerated phase CML who displayed rising white blood cell (WBC) counts while receiving 600 mg STI571 (Gleevec; Novartis, Basel, Switzerland) per day. These studies have been sanctioned by the institutional review board of Virginia Commonwealth University/Medical College of Virginia. Blood was collected into heparinzed syringes, diluted 1:3 with RMPI 1640 medium, and transferred as an overlayer to centrifuge tubes containing 10 mL Ficoll-Hypaque (specific gravity, 1.077-1.081; Sigma, St Louis, MO). After centrifugation at room temperature for 30 minutes, the interface layer, containing mononuclear cells, was extracted with a sterile Pasteur pipette, suspended in RPMI medium, and washed 3 times. CD34$^+$ cells were then isolated using a Miltenyi microbead separation system (Miltenyi BioTech, Auburn, CA) per the manufacturer's instructions. The CD34$^+$ cells were then diluted into RPMI medium containing 10% fetal calf serum at a concentration of 2×10^5 cells/mL, and exposed to drugs as described in the case of K562 cells.

Reagents

Sodium butyrate (SB), SAHA, SP600125, and JNK inhibitor I were supplied by Calbiochem (San Diego, CA). BOC-fmk and IETD-fmk were purchased from Enzyme Products (Livermore, CA). All were formulated in sterile dimethyl sulfoxide (DMSO) before use. L-N-acetylcyteine (LNAC), roscovitine, and MG132 were purchased from Sigma and formulated in sterile medium. Bortezomib was kindly provided by Sarah Waywell, Millennium Pharmaceuticals (Cambridge MA). Annexin V/propidium iodide (PI) was supplied by BD PharMingen (San Diego, CA) and formulated per the manufacturer's instructions. Dichlorohydrofluoroscein diacetate, di(acetoxymethyl ester) (DCF) was purchased from Molecular Probes (Eugene OR) and formulated in methanol.

Experimental format

Logarithmically growing cells were placed in sterile plastic T-flasks (Corning, Corning, NY) to which the designated drugs were added. The flasks were then placed in a 5% CO_2, 37°C incubator for various intervals. At the end of the incubation period, cells were transferred to sterile centrifuge tubes, pelleted by centrifugation at 400*g* for 10 minutes at room temperature, and prepared for the corresponding analysis.

Assessment of apoptosis

After drug exposures, cytocentrifuge preparations were stained with Wright-Giemsa and viewed by light microscopy to evaluate the extent of apoptosis as described previously.[30] For each condition, 10 to 15 randomly selected fields, encompassing more than 700 cells, were scored. To confirm the results of morphologic analysis, flow cytometric analysis of annexin V/PI-stained cells was performed as described previously.[29] In all studies, the results of morphologic assessment and annexin V/PI staining yielded highly concordant results.

Preparation of S-100 fractions and assessment of cytochrome *c* release

K562 cells were harvested after drug treatment and cytosolic S-100 fractions were prepared as described in detail previously.[30] Western blot analysis assessing cytochrome *c* release was performed as described in the next section.

Immunoblot analysis

Immunoblotting was performed as described previously.[30] The sources of primary antibodies were as follows: Bcl-x_L, rabbit polyclonal (Santa Cruz Biotechnology, Santa Cruz, CA); X-linked inhibitor of apoptosis protein (XIAP), rabbit polyclonal (R & D Systems, Minneapolis, MN); Mcl-1, mouse monoclonal (BD PharMingen); cyclin D1, mouse monoclonal (PharMingen); p27, mouse monoclonal (PharMingen); extracellular signal-related kinase 1/2 (ERK 1/2), rabbit polyclonal (Cell Signaling Technology, Beverly, MA); phospho-ERK 1/2 (thr202/tyr204), rabbit polyclonal (Cell Signaling Technology); phospho-MEK, rabbit polyclonal (Cell Signaling Technology); phospho-JNK, mouse monoclonal (Santa Cruz Biotechnology); Raf1, mouse monoclonal (Santa Cruz Biotechnology); apoptosis-inducing factor (AIF), mouse monoclonal (Santa Cruz Biotechnology); Flice inhibitory protein (FLIP), mouse monoclonal (Santa Cruz Biotechnology); cellular inhibitor of apoptosis protein 1 (cIAP1) mouse monoclonal (Santa Cruz Biotechnology); cIAP2, mouse monoclonal (Santa Cruz Biotechnology); Bax, mouse monoclonal (Santa Cruz Biotechnology); c-Abl, mouse monoclonal (Santa Cruz Biotechnology); phospho-p38 mitogen-activated protein kinase (MAPK), rabbit polyclonal (Cell Signaling Technology); cytochrome *c*, mouse monoclonal; caspase-3, mouse monoclonal (Transduction Laboratories, Lexington, KY); p21, mouse monoclonal

(Transduction Laboratories); poly(adenosine diphosphate–ribose) polymerase (PARP, C-2-10), mouse monoclonal (BioMol Research Laboratories, Plymouth, MA); and second mitochondria-derived activator of caspase (Smac), rabbit polyclonal (Upstate Biotechnology, Lake Placid, NY). Blots were washed 3 × 15 minutes in Tris (tris(hydroxymethyl)aminomethane)–buffered saline/Tween 20 (TBS-T) and then incubated with a 1:2000 dilution of horseradish peroxidase–conjugated secondary antibody (Bio-Rad Laboratories, Hercules, CA) for 1 hour at 22°C. Blots were again washed 3 × 15 minutes in TBS-T and then developed by enhanced chemiluminescence (Pierce, Rockford, IL).

Transient transfections

Plasmids encoding enhanced green fluorescence protein (EGFP) under the transcriptional control of the human cytomegalovirus (CMV) immediate-early promoter (pEGFP-C2) and hemagluttinin (HA)–tagged activated MEK1 (S218D/S222D in pUSEamp) were obtained from Clontech Laboratories (Palo Alto, CA) and Upstate Biotechnology, respectively. A 1285–base pair (bp) fragment containing the *MEK1* cDNA was obtained by *Apa*I and partial *Eco*RI digestion and inserted in-frame into the (C-terminal) multiple cloning site of pEGFP-C2. The entire *MEK1* cDNA in the fusion construct was sequenced and the reading frame was confirmed. Log-phase K562 cells were transfected in electroporation hypo-osmolar buffer (Eppendorf, Westbury, NY) using a BTX electromanipulator 600 (Eppendorf). DNA (20 μg) and 2.0×10^7 cells were used for each condition. After 12 hours of incubation, 20% to 30% of the cells displayed green fluorescence. The brightest 10% to 20% of the total cell population was isolated by fluorescence-activated cell sorting (FACS) using a Cytomation MoFLO cell sorter (Ft Collins, MO). The cells were then exposed to drugs as indicated, and examined for evidence of apoptosis by the methods described in "Assessment of apoptosis."

Determination of reactive oxygen species (ROS)

Following treatment, cells were incubated with 1 μg/mL DCF for 30 minutes, after which they were washed thoroughly in phosphate-buffered saline, and the percentage of cells displaying increased dye uptake, reflecting an increase in ROS levels, was determined using a Becton Dickinson FACScan flow cytometer (Hialeah, FL) in conjunction with Cell Quest 3.2 software (Becton Dickinson).

Electrophoretic mobility shift assay (EMSA)

Nuclear extracts were prepared as described previously.[31] Double-stranded oligonucleotides corresponding to NF-κB binding site of immunoglobulin κ (Igκ) promoter 5′-AGTTGAGGGGACTTTCCCAGGC-3′ were obtained from Promega (Madison, WI) and labeled with [γ^{32}P] adenosine triphosphate (3000 Ci/mmol [111 000 MBq/mmol]; ICN Biomedicals, Irvine, CA) using T4 polynucleotide kinase (Promega) and purified using G-25 column (Amersham Pharmacia Biotech, Piscataway, NJ). Nuclear extracts (5 μg) were incubated at 4°C for 20 minutes with 10^5 cpm of labeled oligonucleotide probe dissolved in 15 μL binding buffer (20 mM HEPES [*N*-2-hydroxyethylpiperazine-*N*′-2-ethanesulfonic acid, pH 7.9] 5 mM $MgCl_2$, 4 mM dithiothreitol, 20% glycerol, 0.1 mM phenylmethylsulfonyl fluoride, 5 mM benzamidine, 2 mM levamisol, 0.1 μg/mL aprotinin, 0.1 μg/mL bestatin, 2 μg poly(dI/dC)). The reaction mixtures were then loaded onto 6% native polyacrylamide gels in 0.09 M Tris borate, 2 mM EDTA (ethylenediaminetetraacetic acid), and pH 8.0 buffer, and electrophoresed for 2 hours at 150 V. The gels were dried at 80°C and exposed to X-ray film for autoradiography.

For quantitation of DNA binding activity, autoradiograms were scanned and densitometric analysis was performed using a FluorChem 8800 densitometer (Alpha Innotech, San Leandro, CA) and accompanying program.

Statistical analysis

The significance of differences between experimental conditions was determined using the 2-tailed Student *t* test. Characterization of synergistic and antagonistic interactions was performed using median dose effect analysis in conjunction with a commercially available software program (CalcuSyn; Biosoft, Ferguson, MO).[32]

Results

The proteasome inhibitor bortezomib interacts synergistically with SAHA to induce apoptosis in Bcr/Abl$^+$ K562 cells

To determine what effect, if any, bortezomib would exert on the response of K562 cells to the HDIs SAHA and SB, cells were exposed for 48 hours to 1.5 μM SAHA ± the indicated concentrations of bortezomib, after which the percentage of apoptotic cells was determined as described in "Materials and methods." Treatment of cells with SAHA and bortezomib alone was minimally toxic to these cells (Figure 1A). However, when SAHA was combined with bortezomib concentrations 3 nM or higher, a marked increase in cell death was observed, which was virtually complete for bortezomib concentrations higher than 5 nM. Identical results were obtained using multiple methods for assessing apoptosis (eg, annexin V/PI and 7-amino-actinomycin-D uptake; data not shown). A parallel SAHA dose-response curve revealed that coadministration of SAHA at concentrations 1.0 μM or higher in conjunction with a nontoxic concentration of bortezomib (4.5 nM) resulted in a marked increase in cell death, which approached 100% at higher SAHA concentrations (Figure 1B). Median dose effect analysis of interactions between SAHA and bortezomib yielded combination index values considerably less than 1.0,

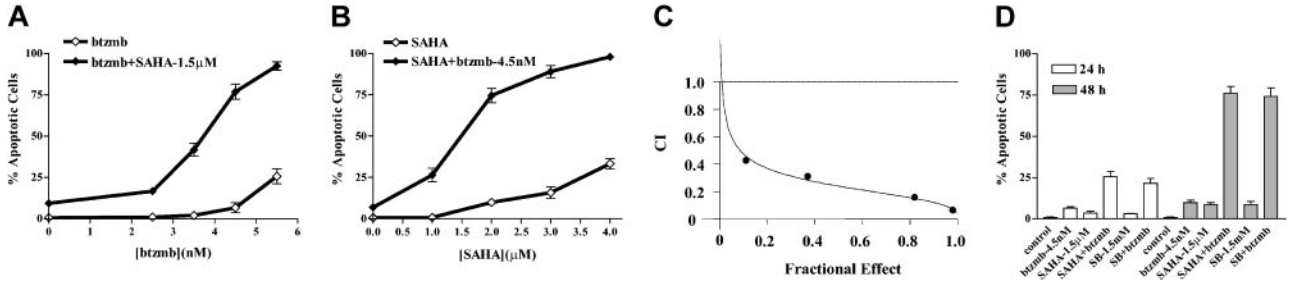

Figure 1. Induction of apoptosis in K562 cells by SAHA or SB and bortezomib. (A) K562 cells were exposed for 48 hours to 1.5 μM SAHA in conjunction with the indicated concentration of bortezomib (btzmb), after which apoptosis was monitored by morphologic analysis of Wright Giemsa–stained specimens as described in "Materials and methods." (B) Cells were exposed for 48 hours to 4.5 nM bortezomib in conjunction with the designated concentration of SAHA, after which apoptosis was assessed as above. (C) K562 cells were exposed to varying concentrations of SAHA and bortezomib at a fixed ratio (333:1) for 48 hours after which combination index (CI) values for apoptosis were determined in relation to the fraction affected (FA) using median dose effect analysis. CI values less than 1.0 correspond to a synergistic interaction. (D) K562 cells were exposed to 1.5 μM SAHA ± 4.5 nM bortezomib for the indicated intervals, after which the percentage of apoptotic cells was assessed as described in "Materials and methods." In each case, values represent the means ± SD for 3 separate experiments.

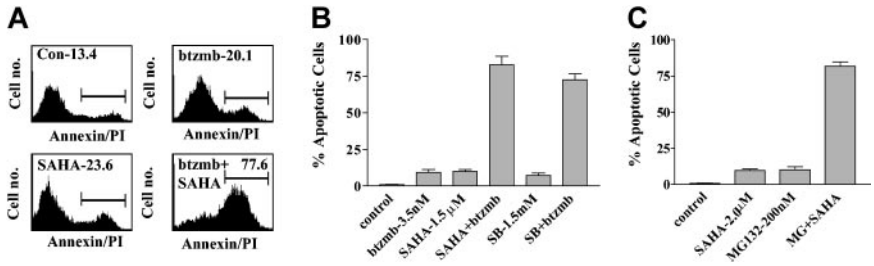

Figure 2. Induction of apoptosis in LAMA 84 cells by SAHA or SB and bortezomib. (A) LAMA 84 cells were exposed to 4.5 nM bortezomib ± 1.5 μM SAHA for 48 hours, after which the percentage of annexin V/PI$^+$ cells (shown above gated area) was determined by flow cytometry as described in "Materials and methods." An additional 2 studies yielded equivalent results. (B) Cotreatment of LAMA 84 cells with 3.5 nM bortezomib and 1.5 μM SAHA or 1.5 mM sodium butyrate (SB) for 48 hours, after which the percentage of apoptotic cells was assessed as described in "Materials and methods." (C) K562 cells were exposed to 2.0 μM SAHA ± 200 nM MG132 for 48 hours, after which the percentage of apoptotic cells was assessed as described in "Materials and methods." In each case, values represent the means ± SD for 3 separate experiments.

denoting highly synergistic interactions (Figure 1C). The data in Figure 1D indicate that enhanced apoptosis in cells treated with PS-241 + HDIs could be detected after 24 hours of exposure, and increased substantially over the ensuing 24 hours. In addition, bortezomib also interacted synergistically with another HDI (SB; 1.5 mM) to trigger cell death in K562 cells. Together, these findings indicate that combinations of minimally toxic concentrations of bortezomib with several HDIs are effective in inducing cell death in Bcr/Abl$^+$ cells.

In separate studies, coadministration of comparable concentrations of bortezomib and either SB or SAHA resulted in a similar potentiation of apoptosis in Bcr/Abl$^-$ human leukemia cell types, including U937 myelomonocytic, HL-60 promyelocytic, and Jurkat lymphoblastic leukemia cells (data not shown), indicating that expression of the Bcr/Abl kinase was not required for antileukemic synergism between these agents.

Bortezomib interacts synergistically with HDIs to induce apoptosis in Bcr/Abl$^+$ LAMA 84 cells

To establish whether these interactions were restricted to K562 cells or could be extended to other Bcr/Abl$^+$ leukemia cell types, parallel studies were carried out in LAMA 84 cells (Figure 2). The results of flow cytometric analysis shown in Figure 2A demonstrate that 48-hour exposure of LAMA 84 cells to 3.5 nM bortezomib or 1.5 μ SAHA individually resulted in 20.1% and 23.7% annexin V/PI$^+$ cells, respectively, whereas combined treatment resulted in 77.7% annexin V/PI$^+$ cells (Figure 2A). Data shown in Figure 2B revealed that coadministration of 1.5 mM SB with bortezomib led to a marked increase in apoptosis in LAMA 84 cells, similar to results obtained in K562 cells (Figure 1). These findings demonstrate that synergistic interactions between bortezomib and HDIs are not restricted to K562 Bcr/Abl$^+$ leukemic cells.

MG-132 strikingly increases SAHA-mediated lethality in K562 cells

To determine whether proteasome inhibitors other than bortezomib could potentiate HDI-mediated lethality in Bcr/Abl$^+$ cells, K562 cells were exposed for 48 hours to 2.0 μM SAHA ± the proteasome inhibitor MG-132 (200 nM). While the agents administered individually minimally induced apoptosis (ie, < 10%), combined treatment yielded approximately 65% cell death (Figure 2C). Such findings suggest that this phenomenon is not restricted to bortezomib, but can be extended to other classes of proteasome inhibitors.

Coadministration of bortezomib and HDIs in Bcr/Abl$^+$ cells results in enhanced activation of caspases-9, -3, and -8, PARP cleavage, Bcr/Abl down-regulation, and release of cytochrome *c*, Smac/DIABLO, and AIF into the cytosolic S-100 fraction

Western analysis was subsequently used to assess the effects of combining bortezomib with SAHA or SB on various apoptosis-associated events in K562 cells (Figure 3). Whereas treatment of cells with bortezomib, SB, or SAHA alone exerted minimal effects, coadministration of bortezomib with SAHA or SB resulted in a dramatic increase in caspases-9, -3, and -8 processing, as well as PARP degradation. Combined treatment with bortezomib and SAHA or SB also resulted in marked down-regulation of the Bcr/Abl protein levels, as well as a striking increase in release of the proapoptotic mitochondrial proteins cytochrome *c*, Smac/DIABLO,

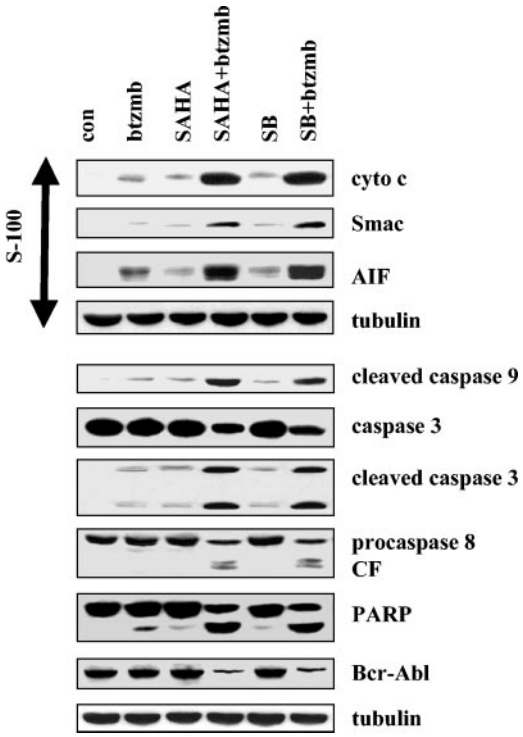

Figure 3. Induction of mitochondrial injury and caspase activation in K562 cells by SAHA or SB and bortezomib. K562 cells were exposed to 1.5 μM SAHA ± 4.5 nM bortezomib for 48 hours, after which Western analysis was used to assess release of AIF, Smac/DIABLO, and cytochrome *c* into S-100 cytosolic fractions, and total cellular extracts were monitored for expression of cleaved caspase-9, caspase-3, caspase-8, PARP, and Bcr/Abl. Each lane contained 25 μg protein; blots were stripped and reprobed for tubulin to ensure equivalent loading and transfer. An additional 2 studies yielded equivalent results.

and AIF into the cytosolic S-100 fraction. Together, these findings indicate that coadministration of bortezomib and HDIs represents a very potent stimulus for mitochondrial injury and caspase activation in Bcr/Abl$^+$ leukemic cells.

Bortezomib + HDIs up-regulate expression of the antiapoptotic protein Mcl-1 in K562 cells

The prosurvival actions of the Bcr/Abl kinase have been associated with altered expression of antiapoptotic proteins, including Bcl-xL and XIAP.[5] Consequently, studies were performed to determine whether the bortezomib/HDI regimen modified expression of these proteins (Figure 4). Administration of bortezomib, SB, or SAHA individually or in combination (24 hours) exerted minimal effects on the expression of Bcl-xL, XIAP, c-IAP1, c-IAP2, or FLIP. Combined treatment with SB or SAHA with bortezomib did, however, result in decline in levels of full-length Bid, presumably corresponding to cleavage/activation. This finding may be particularly relevant in view of evidence implicating Bid activation in SAHA-mediated lethality.[23] Interestingly, treatment of K562 cells with bortezomib resulted in an increase in Mcl-1 levels, an effect that was unperturbed by coadministration of either SAHA or SB. Thus, coadministration of bortezomib and HDIs failed to down-regulate expression of antiapoptotic Bcl-2 family members, suggesting that the lethal effects of this drug combination are not specifically related to abrogation of Bcr/Abl downstream events.

Bortezomib and HDIs promote p21^{CIP1} accumulation and cleavage, cyclin D_1 down-regulation, and pRb degradation

To determine what effect combined exposure of K562 cells to proteasome and histone deacetylase inhibitors would have on

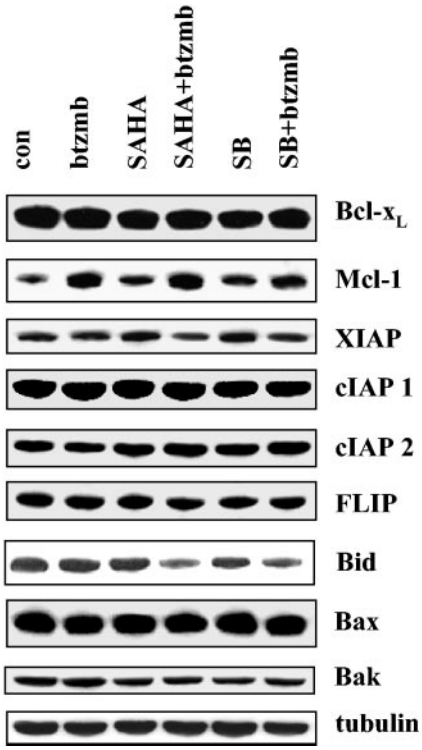

Figure 4. Effects of SAHA or SB and bortezomib on Bcl-2 family members in K562 cells. K562 cells were exposed to 1.5 μM SAHA ± 4.5 nM bortezomib for 24 hours, after which Western analysis was used to assess expression of Bcl-x_L, Mcl-1, XIAP, cIAP1, cIAP2, FLIP, Bax, Bak, and full-length Bid. Each lane contained 25 μg protein; blots were stripped and reprobed for tubulin to ensure equivalent loading and transfer. An additional 2 studies yielded equivalent results.

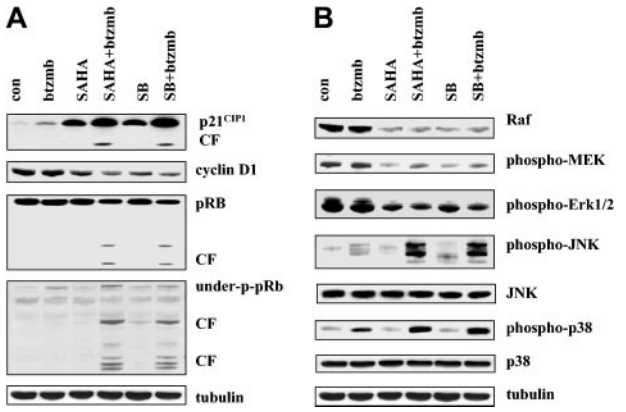

Figure 5. Effects of SAHA or SB and bortezomib on cell cycle and signaling protein K562 cells. (A) K562 cells were exposed to 1.5 μM SAHA ± 4.5 nM bortezomib for 24 hours, after which the expression of p21^{CIP1}, cyclin D_1, total pRb, and underphosphorylated pRb were examined by Western blot as described in "Materials and methods." CF indicates cleavage fragment. Each lane contained 25 μg protein. (B) Following treatment with SAHA ± bortezomib as shown in panel A, expression of Raf, phospho-MEK1/2 and phospho-ERK1/2, phospho-JNK, total JNK, phospho-p38 MAPK, and total p38 was monitored as in panel A. Each lane contained 25 μg protein; blots were stripped and reprobed for tubulin to ensure equivalent loading and transfer. An additional 2 studies yielded equivalent results.

various cell cycle regulatory proteins, cells were exposed for 24 hours to 4.5 nM bortezomib ± 1.5 mM SB or 1.5 μM SAHA, after which expression of p21^{CIP1}, cyclin D_1, and phosphorylation of the retinoblastoma protein (pRb) was monitored by Western analysis (Figure 5). As previously reported,[22] SB and SAHA robustly induced p21^{CIP1}, whereas effects of bortezomib were considerably less pronounced (Figure 5A). However, cells exposed to bortezomib + SB or SAHA displayed a further increase in p21^{CIP1} induction, as well as evidence of a p21^{CIP1} cleavage fragment. While bortezomib alone failed to modify cyclin D_1 levels, both SAHA and SB induced down-regulation of this protein. Moreover, combined treatment of cells with bortezomib + HDIs resulted in further down-regulation of cyclin D_1. Finally, exposure of cells to bortezomib + HDIs (but not to these agents administered alone) resulted in cleavage of full-length and underphosphorylated pRb. Thus, coadministration of bortezomib and HDIs in K562 cells was associated with induction and cleavage of p21^{CIP1}, down-regulation of cyclin D_1, and degradation of pRb.

Exposure of K562 cells to bortezomib and HDIs redirects signals away from cytoprotective and toward stress-related MAPK pathways

Effects of combined exposure of K562 cells were then examined in relation to perturbations in the outputs of cytoprotective- and stress-related MAP kinase signaling modules (Figure 5B). While bortezomib (4.5 nM) alone had little effect, exposure of cells for 24 hours to SAHA (1.5 μM) or SB (1.5 mM), with or without bortezomib, reduced Raf-1 expression as well as that of phospho-MEK and phospho-ERK. Levels of total MEK and ERK were unchanged (data not shown). However, whereas each of the agents administered individually exerted little effect on levels of phospho-JNK, combined treatment resulted in a striking increase in JNK activation. Total JNK levels were unchanged under all treatment conditions. Lastly, bortezomib alone modestly activated p38 MAPK, whereas HDIs exerted minimal effects. However, combined treatment with bortezomib and each of the HDIs resulted in a marked increase in phosphorylation of p38 MAPK. Collectively, these findings indicate that combined exposure of K562 cells to bortezomib and HDIs markedly shifts signaling toward the JNK and

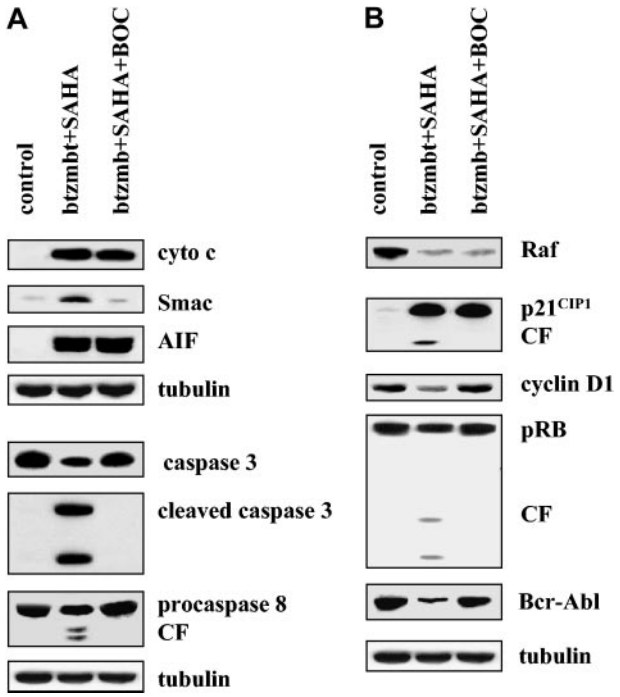

Figure 6. Caspase dependence of SAHA/bortezomib effects in K562 cells. (A) K562 cells were exposed to 1.5 μM SAHA + 4.5 nM bortezomib for 36 hours in the presence or absence 25 μM BOC-fmk, after which release of cytochrome *c* or Smac/DIABLO or AIF into the S-100 cytosolic fraction and the expression of procaspase-3, cleaved caspase-3, and procaspase-8 in total cell lysates were assessed as described in "Materials and methods." (B) Cells were treated with SAHA + bortezomib ± BOC-fmk, after which Western blot analysis was used to assess expression of Raf-1, $p21^{CIP1}$, cyclin D_1, pRb, and Bcr-Abl. CF indicates cleavage fragment. Each lane contained 25 μg protein; blots were stripped and reprobed for tubulin to ensure equivalent loading and transfer. An additional 2 studies yielded equivalent results.

p38 MAPK stress-related pathways and away from the cytoprotective Raf/MEK/ERK cascade.

Bortezomib/SAHA-mediated cytochrome *c* and AIF release and Raf-1 down-regulation is caspase-independent, whereas Smac/DIABLO release, $p21^{CIP1}$ and pRb degradation, and down-regulation of cyclin D_1 and Bcr/Abl are caspase-dependent

To determine which of these events represented a consequence of bortezomib/HDI-mediated caspase activation, cells were exposed for 24 hours to 4.5 nM bortezomib and 1.5 μM SAHA in the presence or absence of the pancaspase inhibitor Boc-D-fmk (20 μM), after which expression of various proteins was monitored by Western analysis (Figure 6). Under these conditions, addition of Boc-D-fmk reduced bortezomib/SAHA-mediated apoptosis from 68 ± 6% to 17 ± 5% (data not shown). As shown in Figure 6A, Boc-D-fmk blocked bortezomib/SAHA-mediated Smac/DIABLO release and processing of caspases-3 and -8, indicating that these represent secondary events. In contrast, release of cytochrome *c* and AIF into the S-100 fraction was undiminished in the presence of Boc-D-fmk, indicating that these events occur upstream of caspase activation. In addition, bortezomib/SAHA-mediated down-regulation of Raf-1 (as well as phospho-MEK and phosphor-ERK; data not shown) was not altered by Boc-D-fmk (Figure 6B). In contrast, cleavage of $p21^{CIP1}$ and pRb, as well as cyclin D_1 and Bcr/Abl down-regulation were largely prevented by addition of the pancaspase inhibitor. These findings indicate that the perturbations in signaling and cell cycle proteins observed in bortezomib/HDI-treated cells occur through both caspase-dependent and -independent mechanisms.

Constitutively active MEK protects K562 cells from bortezomib/SAHA-mediated lethality

To determine whether the down-regulation/inactivation of the Raf/MEK/ERK pathway contributed functionally to proteasome/histone deacetylase inhibitor-mediated lethality, the effects of this regimen were examined in K562 cells transiently transfected with a constitutively active MEK construct that also encoded a GFP protein. Following transfection, GFP-expressing cells were sorted using a Cytomation cell sorter, which routinely yielded populations that were more than 95% viable and more than 96% positive for GFP. Cells transfected with constitutively active MEK/GFP or GFP alone controls were then exposed to 4.5 nM bortezomib + 1.5 μM SAHA for 24 hours, after which the percentage of annexin V/PI^+ cells was determined by flow cytometry. As shown in Figure 7, expression of constitutively active MEK significantly, albeit partially, protected cells from the bortezomib/SAHA regimen ($P < .005$ vs GFP controls). This finding is consistent with the notion that down-regulation of the Raf/MEK/ERK pathway contributes functionally to enhanced apoptosis in bortezomib/HDI-treated cells.

ROS generation plays a critical role in bortezomib/HDI-mediated JNK activation, induction of $p21^{CIP1}$, and apoptosis in K562 cells

In view of evidence that the reactive oxygen species may play an important role in HDI-associated lethality,[23] the effects of combining bortezomib and SAHA on ROS generation were examined using the free radical scavenger L-N-acetylcysteine (LNAC).[33] As shown in Figure 8A, SAHA (1.5 μM) and bortezomib (4.5 nM) administered alone exerted minimal effects of ROS generation, whereas combined treatment resulted in a substantial increase in ROS levels. Furthermore, the latter effect was largely abrogated by coadministration of 15 mM LNAC. Significantly, this event was

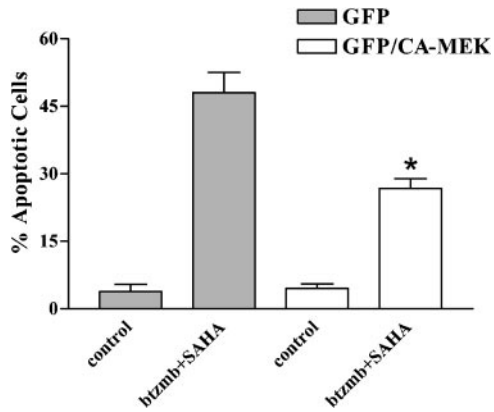

Figure 7. Effect of enforced MEK activation on SAHA/bortezomib-induced apoptosis in K562 cells. K562 cells were transiently transfected, and GFP-expressing cells were isolated using a Cytomation fluorescence-activated cell sorter as described in "Materials and methods." Sorted cells transfected with either GFP alone or the GFP/constitutively active MEK1 fusion cDNA were cultured in drug-free medium for 5 hours, and then exposed to 1.5 μM SAHA ± 4.5 nM bortezomib for 36 hours, after which apoptosis was monitored by examining Wright Giemsa–stained cytospin preparations as described. Values represent the means ± SD for 2 separate determinations. *Significantly less than values for cells transfected with GFP alone; $P < .05$.

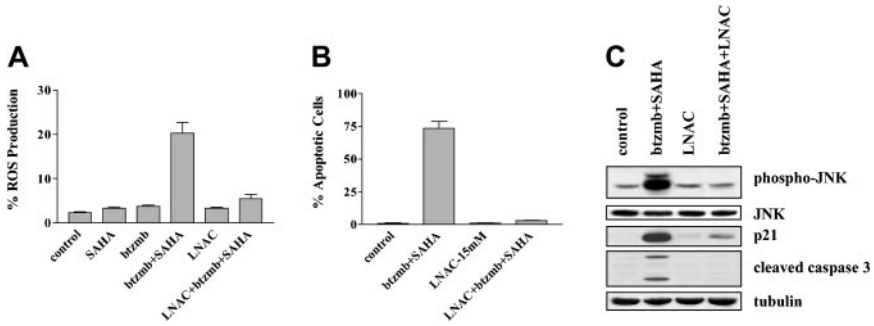

Figure 8. Effect of the antioxidant LNAC on the response of K562 cells to SAHA and bortezomib. (A) K562 cells were exposed to 1.5 μM SAHA ± 4.5 nM bortezomib in the presence or absence of 15 mM LNAC for 4 hours, after which ROS production was assayed by monitoring the percentage of cells displaying increased uptake of dichlorohydrofluoroscein diacetate (DCF) as described in "Materials and methods." (B) Cells were treated with SAHA + bortezomib as shown in panel A ± 15 mM LNAC for 24 hours, after which the percentage of apoptotic cells was determined by examining Wright Giemsa–stained specimens under light microscopy as described in "Materials and methods." For panels A-B, values represent the means ± SD for 3 separate experiments. (C) K562 cells were exposed to 4.5 nM bortezomib + 1.5 μ SAHA for 24 hours in the presence or absence of 15 mM LNAC, after which Western analysis was used to assess expression of JNK, phospho-JNK, $p21^{CIP1}$, and cleaved caspase-3. Each lane contained 25 μg protein; blots were stripped and reprobed for tubulin to ensure equivalent loading and transfer. An additional 2 studies yielded equivalent results.

accompanied by an essentially complete reversal of toxicity (Figure 8B). Interestingly, coadministration of LNAC also blocked bortezomib/SAHA-induced caspase-3 cleavage, JNK phosphorylation, and $p21^{CIP1}$ induction in these cells (Figure 8C). Such findings suggest that ROS generation plays a significant role in the lethality of the bortezomib/HDI regimen toward Bcr/Abl^+ cells, and that in this process, oxidative stress lies upstream of JNK and $p21^{CIP1}$ induction.

Disruption of the NF-κB pathway by bortezomib and Bay 11-7082 is associated with potentiation of SAHA-mediated apoptosis in K562 cells

EMSA analysis was then used to assess the effects of bortezomib on NF-κB activity in SAHA-treated K562 cells. As shown in Figure 9A, whereas exposure of cells to SAHA alone (one hour) resulted in a very small decrease in NF-κB DNA binding, exposures to bortezomib and particularly the combination of SAHA and bortezomib were associated with substantial declines. Quantitation of NF-κB DNA binding by densitometry (Figure 9B) revealed reductions of 40% and 50% in DNA binding activity for SAHA and SAHA/bortezomib ($P < .01$ and .005 versus control, respectively). In addition, coexposure (48 hours) of K562 cells to SAHA (2.0 μM) and the NF-κB inhibitor Bay 11-7082 (3.0 μM) resulted in a marked increase in apoptosis, an effect mimicking interactions between SAHA and bortezomib (Figure 9B). Together, these findings are consistent with the notion that disruption of the NF-κB pathway by bortezomib lowers the threshold for HDI-mediated apoptosis in K562 cells.

The bortezomib/HDI regimen effectively induces apoptosis in continuously cultured as well as primary Bcr/Abl^+ cells resistant to STI571

To determine whether Bcr/Abl^+ cells resistant to STI571 would be sensitive to this strategy, a multidrug-resistant cell line (K562R), which has previously been shown to express increased levels of the Bcr/Abl protein and display marked resistance to STI571,[29] was used. As shown in Figure 10A, 48-hour exposure of cells to bortezomib and either SAHA or SB, at concentrations that induced only modest toxicity when the agents were administered alone, resulted in a marked increase in apoptosis in each case (ie, ~75%). Parallel studies were performed using $CD34^+$ mononuclear cells obtained from the peripheral blood of a patient with CML in accelerated phase who was experiencing increasing WBC counts while receiving 600 mg of STI571/d. Whereas 48-hour exposure of such cells to 5 nM bortezomib or 2.0 μM SAHA individually induced only a small amount of apoptosis, combined treatment resulted in approximately 75% cell death, analogous to results obtained in continuously cultured cell lines. In contrast, this drug combination was associated with only minimal toxicity (ie, < 20% apoptosis) in normal peripheral blood mononuclear cells (data not shown). These findings raise the possibility that at least certain types of STI571-resistant Bcr/Abl^+ cells remain susceptible to the strategy of combining bortezomib with clinically relevant HDIs.

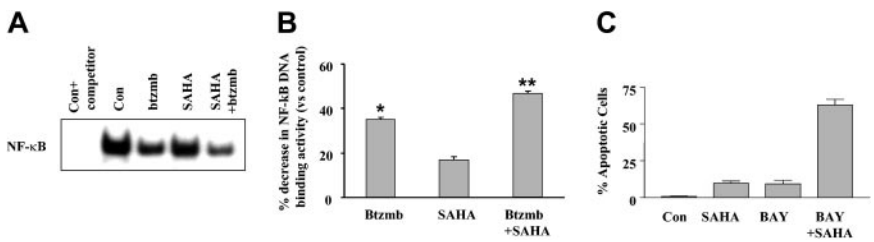

Figure 9. Effect of SAHA and bortezomib on NF-κB activation in K562 cells. (A) K562 cells were exposed to 1.5 μM SAHA ± 4.5 nM bortezomib for one hour, after which EMSA analysis was used to monitor NF-κB DNA binding as described in "Materials and methods." The first lane corresponds to control extracts exposed to an unlabeled competitor to exclude nonspecific DNA binding. (B) NF-κB DNA binding activity was quantified densitometrically as described in "Materials and methods," and values for each condition were expressed in relation to untreated controls. Values represent the means for triplicate determinations ± SEM. $P < .01$ (*) or $< .005$ (**) relative to untreated controls. (C) K562 cells were exposed to SAHA (2.0 μM) ± the NF-κB inhibitor BAY 11-7082 for 48 hours, after which the percentage of apoptotic cells was determined by examining Wright Giemsa–stained specimens under light microscopy as described in "Materials and methods." Values represent the means ± SD for 3 separate experiments performed in triplicate.

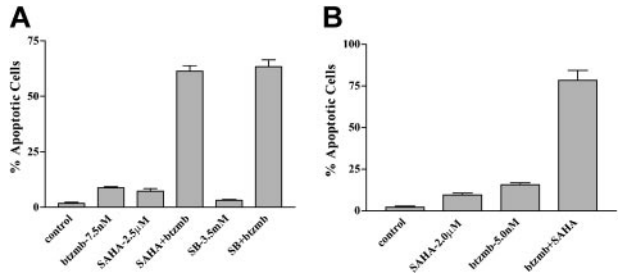

Figure 10. Effect of SAHA and bortezomib on apoptosis in STI571-resistant K562 and patient-derived CD34$^+$ cells. (A) STI571-resistant K562R cells were exposed to 7.5 nM bortezomib ± either 2.5 μM SAHA or 3.5 mM SB for 48 hours, after which the percentage of apoptotic cells was determined by examination of Wright Giemsa–stained cytospin preparations under light microscopy as described in "Materials and methods." Values represent the means ± SD for 3 separate experiments performed in triplicate. (B) CD34$^+$ cells were isolated from the peripheral blood of a patient with accelerated phase CML who experienced progressive disease while receiving STI571 and exposed to 2.0 μM SAHA ± 5.0 nM bortezomib for 48 hours. The percentage of apoptotic cells was then determined by examination of Wright Giemsa–stained cytospin preparations as shown in panel A. Values represent the means ± for 12 randomly selected fields encompassing more than 1000 cells.

Discussion

The present studies indicate that coadministration of the proteasome inhibitor bortezomib with clinically relevant HDIs potently induces mitochondrial damage (eg, cytochrome *c*, Smac/DIABLO, and AIF release), caspase activation, and apoptosis in Bcr/Abl$^+$ leukemia cells, as well as in their Bcr/Abl$^-$ counterparts, and that these events are associated with multiple perturbations in survival, signaling, and cell cycle regulatory proteins. Such findings are in accord with those of Giuliano et al, who previously described synergistic induction of cytochrome *c* release and apoptosis in Y79 retinoblastoma cells exposed to the proteasome inhibitor MG-132 in combination with SB.[34] Because the constitutively active Bcr/Abl kinase signals to multiple downstream cytoprotective targets,[5-9] Bcr/Abl$^+$ cells are classically resistant to apoptosis induced by most conventional cytotoxic agents.[4] However, the marked susceptibility of such cells to bortezomib/HDI-mediated lethality indicates that this regimen is able to circumvent the blockade to mitochondrial injury and caspase activation conferred by the Bcr/Abl kinase, or alternatively, to act at a point downstream of Bcr/Abl cytoprotective actions. The present findings also indicate that leukemia cells in general may be particularly vulnerable to this novel strategy.

Several lines of evidence suggest that enhanced lethality of the bortezomib/HDI combination stems, at least in part, from a redirection of signals away from cytoprotective and toward stress-related cascades. For example, in PC12 cells, the net output of the JNK and ERK pathways determines whether cells live or die in response to growth factor deprivation.[35] Furthermore, JNK activation has been implicated in events associated with mitochondrial damage and cytochrome *c* release.[36] For these reasons, activation of stress-related cascades is one of the factors thought to be involved in proteasome inhibitor-mediated lethality.[37] Moreover, interference with MEK/ERK signaling (ie, by pharmacologic MEK inhibitors) has recently been shown to promote the lethal actions of proteasome inhibitors.[38] It is noteworthy that exposure of K562 cells to HDIs resulted in down-regulation of the Raf/MEK/ERK cascade, in agreement with previous reports demonstrating similar events in depsipeptide-treated non–small cell lung cancer cells.[39] Significantly, enforced activation of MEK/ERK partially protected K562 cells from bortezomib/HDI-mediated apoptosis, indicating that interference with this pathway plays a functional role in the lethality of this regimen. However, it is also important to note that subtoxic HDI concentrations also induced down-regulation of the Raf/MEK/ERK cascade, suggesting that such actions may be necessary but not sufficient to induce cell death. On the other hand, inactivation of ERK (ie, by HDIs), when combined with JNK activation (ie, in cells exposed to proteasome inhibitors), may trigger mitochondrial damage leading to engagement of the apoptotic cascade. Consistent with such a model, we have recently observed that synergistic interactions between HDIs such as SAHA and the Bcr/Abl kinase inhibitor STI571 in Bcr/Abl$^+$ cells involves simultaneous activation of JNK in conjunction with inactivation of the Raf/MEK/ERK pathway.[40] It is worth noting that in accord with the results of Nimmanapalli et al,[41] we also observed that coadministration of SAHA with STI571 potentiated down-regulation of the Bcr/Abl protein,[40] analogous to the actions of SAHA and bortezomib. Thus, HDIs such as SAHA may interact with other novel agents by disrupting multiple cytoprotective signaling pathways and by shifting the balance toward their stress-related counterparts, particularly in Bcr/Abl$^+$ cells.

The observation that enhanced bortezomib/HDI-mediated apoptosis in Bcr/Abl$^+$ cells occurred despite up-regulation of p21^{CIP1} was unexpected in view of evidence that this cyclin-dependent kinase inhibitor has generally been thought to exert antiapoptotic effects,[42] particularly in the case of HDI-related lethality.[22,43] In this setting, increased expression of p21^{CIP1} presumably reflects bortezomib-mediated interference with proteasomal degradation, which plays a key role in regulating abundance of this protein.[44] However, examples of proapoptotic actions of p21^{CIP1} exist.[45] In addition, treatment of cells with bortezomib + HDIs resulted in the appearance of a p21^{CIP1} cleavage product, which has been linked to apoptosis induction.[46] Whether up-regulation of p21^{CIP1} in bortezomib/HDI-treated Bcr/Abl$^+$ cells contributes to lethality or is simply unable to oppose activation of the caspase cascade remains to be determined.

Cotreatment of Bcr/Abl$^+$ cells with bortezomib/HDIs resulted in the caspase-dependent degradation of several proteins associated with antiapoptotic effects, including Bcr/Abl itself,[3] cyclin D_1,[47] and pRb,[48] as well as release of the XIAP inhibitor Smac/DIABLO.[49] While the initial induction of apoptosis by the bortezomib/HDI regimen cannot be attributed to such actions, they may nevertheless serve to amplify activation of the apoptotic cascade once it has been triggered. Interestingly, exposure of cells to bortezomib with or without HDIs resulted in up-regulation of Mcl-1, which has recently been shown to play an important regulatory role in the survival of hematopoietic cells.[50] The present findings indicate that enhanced expression of Mcl-1 is unable to block the proapoptotic actions of the bortezomib/HDI regimen in Bcr/Abl$^+$ cells.

It is noteworthy that coadministration of bortezomib with HDIs resulted in a marked increase in ROS generation of Bcr/Abl$^+$ cells, and that the free radical scavenger LNAC blocked this event as well as apoptosis. These observations suggest that perturbations in redox state play a key role in the lethality of this regimen and are also consistent with results of a previous report relating HDI-mediated cytotoxicity to increased ROS levels.[23] Interestingly, in this report, SAHA-induced ROS increases were associated with cleavage/activation of Bid, a BH3-only Bcl-2 family member known to induce mitochondrial injury. The finding that combined treatment of leukemia cells with HDI/bortezomib also promoted Bid activation (Figure 4) raises the possibility that such an action may have contributed to oxidative stress and apoptosis induced by

this regimen. Another plausible explanation for these events is that the NF-κB pathway, which is known to be involved in protecting cells from oxidative stress,[51] may limit the lethal consequences of HDI-mediated ROS generation. Thus, proteasome inhibitors, by disabling the NF-κB cascade,[19] may lower the threshold for HDI-induced mitochondrial injury and apoptosis. The findings that coadministration of bortezomib diminished NF-κB DNA binding in SAHA-treated K562 cells and that the NF-κB inhibitor Bay 11-7082 mimicked the capacity of bortezomib to potentiate SAHA lethality are consistent with this notion. Interestingly, interference with ROS generation by LNAC also attenuated both JNK activation and $p21^{CIP1}$ induction in cells exposed to the bortezomib/HDI regimen. This suggests that ROS generation operates upstream of JNK activation to trigger mitochondrial damage and apoptosis, possibly in conjunction with down-regulation of the Raf/MEK/ERK cascade. The relationship between LNAC-mediated blockade of $p21^{CIP1}$ induction and these events is unclear, although the recent finding that LNAC-related attenuation of ROS generation blocked $p21^{CIP1}$-associated growth arrest and senescence in normal and neoplastic cells[52] may be relevant.

While the introduction of the Bcr/Abl kinase inhibitor STI571 into the clinical armentarium represents a major advance in the treatment of CML, the development of drug resistance constitutes a major barrier to the cure of this disease. Thus far, the major mechanisms of clinical resistance appear to involve either increased expression of the Bcr/Abl protein through gene amplification[14] or the development of mutations in the Bcr/Abl catalytic domain, which interfere with STI571 binding to Bcr/Abl.[53] The finding that the bortezomib/HDI regimen effectively induced apoptosis in an STI571-resistant K562 cell line displaying increased Bcr/Abl expression[29] raises the possibility that such a drug combination may be of use in patients exhibiting the former type of drug resistance. In this regard, the observation that the bortezomib/SAHA combination also effectively triggered apoptosis in primary $CD34^+$ CML mononuclear cells is noteworthy. Although it is not known whether the cells of this patient harbored resistance-related Bcr/Abl mutations, continuously cultured STI571-resistant cell lines engineered to express such mutations are now available.[54] These lines should help to determine whether resistance to STI571 conferred by Bcr/Abl kinase domain mutations can be circumvented by proteasome/HDI inhibitor-based strategies. It will also be of interest to determine whether the bortezomib/HDI regimen spares normal $CD34^+$ progenitor cells, particularly with respect to preservation of clonogenic potential. Finally, the data presented herein suggest that this strategy does not appear to be specifically related to Bcr/Abl-associated pathways, but may have broader applicability to leukemias in general. Nevertheless, the activity of the HDI/bortezomib regimen against Bcr/Abl^+ cells, which are ordinarily quite resistant to diverse apoptotic stimuli,[4,5] may have particular significance. Given ongoing clinical trials involving HDIs[27] and proteasome inhibitors such as bortezomib,[20] further investigation of this novel combination approach in patients with CML and Bcr/Abl^- leukemias may prove feasible. Accordingly, additional studies examining this approach are currently under way.

References

1. Sawyers CL. Chronic myeloid leukemia. N Engl J Med. 1999;340:1330-1340.
2. McLaughlin J, Chianese E, Witte ON. In vitro transformation of immature hematopoietic cells by the P210 BCR/ABL oncogene product of the Philadelphia chromosome. Proc Natl Acad Sci U S A. 1987;84:6558-6562.
3. McGahon A, Bissonnette R, Schmitt M, Cotter KM, Green DR, Cotter TG. BCR-ABL maintains resistance of chronic myelogenous leukemia cells to apoptotic cell death. Blood. 1994;83:1179-1187.
4. Bedi A, Barber JP, Bedi GC, et al. BCR-ABL-mediated inhibition of apoptosis with delay of G2/M transition after DNA damage: a mechanism of resistance to multiple anticancer agents. Blood. 1995;86:1148-1158.
5. Amarante-Mendes GP, McGahon AJ, Nishioka WK, Afar DE, Witte ON, Green DR. Bcl-2-independent Bcr-Abl-mediated resistance to apoptosis: protectionis correlated with up regulation of Bcl-xL. Oncogene. 1998;16:1383-1390.
6. Gesbert F, Sellers WR, Signoretti S, Loda M, Griffin JD. BCR/ABL regulates expression of the cyclin-dependent kinase inhibitor p27Kip1 through the phosphatidylinositol 3-Kinase/AKT pathway. J Biol Chem. 2000;275:39223-39230.
7. Kang CD, Yoo SD, Hwang BW, et al. The inhibition of ERK/MAPK not the activation of JNK/SAPK is primarily required to induce apoptosis in chronic myelogenous leukemic K562 cells. Leuk Res. 2000;24:527-534.
8. Sonoyama J, Matsumura I, Ezoe S, et al. Functional cooperation among Ras, STAT5, and phosphatidylinositol 3-kinase is required for full oncogenic activities of BCR/ABL in K562 cells. J Biol Chem. 2002;277:8076-8082.
9. Rhodes J, York RD, Tara D, Tajinda K, Druker BJ. CrkL functions as a nuclear adaptor and transcriptional activator in Bcr-Abl-expressing cells. Exp Hematol. 2000;28:305-310.
10. Druker BJ. Perspectives on the development of a molecularly targeted agent. Cancer Cell. 2002;1:31-36.
11. Mow BM, Chandra J, Svingen PA, et al. Effects of the Bcr/abl kinase inhibitors STI571 and adaphostin (NSC 680410) on chronic myelogenous leukemia cells in vitro. Blood. 2002;99:664-671.
12. Kawaguchi Y, Jinnai I, Nagai K, et al. Effect of a selective Abl tyrosine kinase inhibitor, STI571, on in vitro growth of BCR-ABL-positive acute lymphoblastic leukemia cells. Leukemia 2001;15:590-594.
13. Druker BJ, Talpaz M, Resta DJ, et al. Efficacy and safety of a specific inhibitor of the BCR-ABL tyrosine kinase in chronic myeloid leukemia. N Engl J Med. 2001;344:1031-1037.
14. Gorre ME, Sawyers CL. Molecular mechanisms of resistance to STI571 in chronic myeloid leukemia. Curr Opin Hematol. 2002;9:303-307.
15. Almond JB, Cohen GM. The proteasome: a novel target for cancer chemotherapy. Leukemia. 2002;16:433-443.
16. Lin ZP, Boller YC, Amer SM, et al. Prevention of brefeldin A-induced resistance to teniposide by the proteasome inhibitor MG-132: involvement of NF-kappaB activation in drug resistance. Cancer Res. 1998;58:3059-3065.
17. Adams J, Palombella VJ, Sausville EA, et al. Proteasome inhibitors: a novel class of potent and effective antitumor agents. Cancer Res. 1999;59:2615-2622.
18. An B, Goldfarb RH, Siman R, Dou QP. Novel dipeptidyl proteasome inhibitors overcome Bcl-2 protective function and selectively accumulate the cyclin-dependent kinase inhibitor p27 and induce apoptosis in transformed, but not normal, human fibroblasts. Cell Death Differ. 1998;5:1062-1075.
19. Cusack JC Jr, Liu R, Houston M, et al. Enhanced chemosensitivity to CPT-11 with proteasome inhibitor PS-341: implications for systemic nuclear factor-kappaB inhibition. Cancer Res. 2001;61:3535-3540.
20. Orlowski RZ, Stinchcombe TE, Mitchell BS, et al. Phase I trial of the proteasome inhibitor PS-341in patients with refractory hematologic malignancies. J Clin Oncol. 2002;20:4420-4427.
21. Marks P, Rifkind RA, Richon VM, Breslow R, Miller T, Kelly WK. Histone deacetylases and cancer: causes and therapies. Nat Rev Cancer. 2001 1:194-202.
22. Rosato RR, Wang Z, Gopalkrishnan RV, Fisher PB, Grant S. Evidence of a functional role for the cyclin-dependent kinase-inhibitor p21WAF1/CIP1/MDA6 in promoting differentiation and preventing mitochondrial dysfunction and apoptosis induced by sodium butyrate in human myelomonocytic leukemia cells (U937). Int J Oncol. 2001;19:181-191.
23. Ruefli AA, Ausserlechner MJ, Bernhard D, et al. The histone deacetylase inhibitor and chemotherapeutic agent suberoylanilide hydroxamic acid (SAHA) induces a cell-death pathway characterized by cleavage of Bid and production of reactive oxygen species. Proc Natl Acad Sci U S A. 2001; 98:10833-10838.
24. Witt O, Sand K, Pekrun A. Butyrate-induced erythroid differentiation of human K562 leukemia cells involves inhibition of ERK and activation of p38 MAP kinase pathways. Blood. 2000;95:2391-2396.
25. O'Connor O, Kelly W, Wang ES, et al. Clinical development of the histone deacetylase inhibitor suberoylanalide hyroxamic acid (SAHA) in aggressive non-Hodgkin's lymphoma (NHL) and Hodgkin's disease (HD) [abstract]. Blood. 2001; 98:611a.
26. Sandor V, Bakke S, Robey RW, et al. Phase I trial of the histone deacetylase inhibitor, depsipeptide (FR901228, NSC 630176), in patients with refractory neoplasms. Clin Cancer Res. 2002;8:718-728.
27. Gore SD, Weng LJ, Figg WD, et al. Impact of prolonged infusions of the putative differentiating agent sodium phenylbutyrate on myelodysplastic

syndromes and acute myeloid leukemia. Clin Cancer Res. 2002;8:963-970.

28. Yin L, Laevsky G, Giardina C. Butyrate suppression of colonocyte NF-kappa B activation and cellular proteasome activity. J Biol Chem. 2001;276: 44641-44646.
29. Yu C, Krystal G, Varticovksi L, et al. Pharmacologic mitogen-activated protein/extracellular signal-regulated kinase kinase/mitogen-activated protein kinase inhibitors interact synergistically with STI571 to induce apoptosis in Bcr/Abl-expressing human leukemia cells. Cancer Res. 2002;62:188-199.
30. Yu C, Krystal G, Dent P, Grant S. Flavopiridol potentiates STI571-induced mitochondrial damage and apoptosis in BCR-ABL-positive human leukemia cells. Clin Cancer Res. 2002;8:2976-2984.
31. Rahmani M, Peron P, Weitzman J, Bakiri L, Lardeux B, Bernuau D. Functional cooperation between JunD and NF-kappaB in rat hepatocytes. Oncogene. 2001;20:5132-5142.
32. Chou TC, Talalay P. Quantitative analysis of dose-effect relationships: the combined effects of multiple drugs or enzyme inhibitors. Adv Enzyme Regul. 1984;22:27-55.
33. Ghezzi P, Bianchi M, Gianera L, Landolfo S, Salmona M. Role of reactive oxygen intermediates in the interferon-mediated depression of hepatic drug metabolism and protective effect of N-acetylcysteine in mice. Cancer Res. 1985; 45:3444-3447.
34. Giuliano M, Lauricella M, Calvaruso G, et al. The apoptotic effects and synergistic interaction of sodium butyrate and MG132 in human retinoblastoma Y79 cells. Cancer Res. 1999;59:5586-5595.
35. Xia Z, Dickens M, Raingeaud J, Davis RJ, Greenberg ME. Opposing effects of ERK and JNK-p38 MAP kinases on apoptosis. Science. 1995;270: 1326-1331.
36. Tournier C, Hess P, Yang DD, et al. The Bax subfamily of Bcl2-related proteins is essential for apoptotic signal transduction by c-Jun NH(2)-terminal kinase. Mol Cell Biol. 2002; 22:4929-4942.
37. Tacchini L, Dansi P, Matteucci E, Bernelli-Zazzera A, Desiderio MA. Influence of proteasome and redox state on heat shock-induced activation of stress kinases, AP-1 and HSF. Biochim Biophys Acta. 2001;1538:76-89.
38. Orlowski RZ, Small GW, Shi YY. Evidence that inhibition of p44/42 mitogen-activated protein kinase signaling is a factor in proteasome inhibitor-mediated apoptosis. J Biol Chem. 2002;277: 27864-27871.
39. Yu X, Guo ZS, Marcu MG, et al. Modulation of p53, ErbB1, ErbB2, and Raf-1 expression in lung cancer cells by depsipeptide FR901228. J Natl Cancer Inst. 2002;94:504-513.
40. Yu C, Rahmani M, Almenara J, et al. Histone deacetylase inhibitors promote STI571-mediated apoptosis in Bcr/Abl$^+$ human leukemia cells sensitive and resistant to STI571. Cancer Res. 2003; 63:2118-2126.
41. Nimmanapalli R, Fuino L, Stobaugh C, Richon V, Bhalla K. Cotreatment with the histone deacetylase inhibitor suberoylanilide hydroxamic acid (SAHA) enhances imatinib-induced apoptosis of Bcr-Abl-positive human acute leukemia cells. Blood. 2003;101:3236-3239.
42. Asada M, Yamada T, Ichijo H, et al. Apoptosis inhibitory activity of cytoplasmic p21(Cip1/WAF1) in monocytic differentiation. EMBO J. 1999;18: 1223-1234.
43. Vrana JA, Decker RH, Johnson CR, et al. Induction of apoptosis in U937 human leukemia cells by suberoylanilide hydroxamic acid (SAHA) proceeds through pathways that are regulated by Bcl-2/Bcl-XL, c-Jun, and p21CIP1, but independent of p53. Oncogene. 1999;18:7016-7025.
44. Di Cunto F, Topley G, Calautti E, et al. Inhibitory function of p21Cip1/WAF1 in differentiation of primary mouse keratinocytes independent of cell cycle control. Science. 1998;280:1069-1072.
45. Chinery R, Brockman JA, Peeler MO, Shyr Y, Beauchamp RD, Coffey RJ. Antioxidants enhance the cytotoxicity of chemotherapeutic agents in colorectal cancer: a p53-independent induction of p21WAF1/CIP1 via C/EBPbeta. Nat Med. 1997;3:1233-1241.
46. Levkau B, Koyama H, Raines EW, et al. Cleavage of p21Cip1/Waf1 and p27Kip1 mediates apoptosis in endothelial cells through activation of Cdk2: role of a caspase cascade. Mol Cell. 1998; 1:553-563.
47. Nahta R, Iglehart JD, Kempkes B, Schmidt EV. Rate-limiting effects of cyclin D1 in transformation by ErbB2 predicts synergy between herceptin and flavopiridol. Cancer Res. 2002;62:2267-2271.
48. Chau BN, Wang JY. Coordinated regulation of life and death by RB. Nat Rev Cancer. 2003;3:130-138.
49. Chai J, Du C, Wu JW, Kyin S, Wang X, Shi Y. Structural and biochemical basis of apoptotic activation by Smac/DIABLO. Nature. 2000;406:855-862.
50. Zhang B, Gojo I, Fenton RG. Myeloid cell factor-1 is a critical survival factor for multiple myeloma. Blood. 2002;99:1885-1893.
51. Schreck R, Albermann K, Baeuerle PA. Nuclear factor kappa B: an oxidative stress-responsive transcription factor of eukaryotic cells. Free Radic Res Commun. 1992;17:221-237.
52. Macip S, Igarashi M, Fang L, et al. Inhibition of p21-mediated ROS accumulation can rescue p21-induced senescence. EMBO J. 2002 ;21: 2180-2188.
53. Shah NP, Nicoll JM, Nagar B, et al. Multiple BCR-ABL kinase domain mutations confer polyclonal resistance to the tyrosine kinase inhibitor imatinib (STI571) in chronic phase and blast crisis chronic myeloid leukemia. Cancer Cell. 2002;2:117-125.
54. La Rosee P, Corbin AS, Stoffregen EP, Deininger MW, Druker BJ. Activity of the Bcr-Abl kinase inhibitor PD180970 against clinically relevant Bcr-Abl isoforms that cause resistance to imatinib mesylate (Gleevec, STI571). Cancer Res. 2002; 62:7149-7153.